Proceedings of the 2007 American Control Conference
Marriott Marquis Hotel at Times Square
New York City, USA, July 11-13, 2007

Feedback Structures for Vapor Compression Cycle Systems

Michael C. Keir, Andrew G. Alleyne,
Department of Mechanical Science and Engineering
University of Illinois at Urbana-Champaign

***Abstract* - This paper explores the controllability and interconnectedness of input-output relationships in vapor compression cycles. The magnitude of physical coupling between different outputs used in the feedback loop are examined. It is shown that an alternative to the conventional feedback configuration found in the literature has distinct benefits that allow for improved system regulation using simple classical control techniques. A relative gain array analysis technique is shown to be an effective method for identifying proper feedback configurations that maximize the controllability of vapor compression systems.**

I. Introduction

The goal of any air conditioning or refrigeration application is to efficiently move energy from one location to another. The amount of energy that must be moved varies considerably and depends on the desired temperature of the cooled space, the ambient conditions, and the level of internal heat generation within the cooled space. Capacity control methods allow these systems to meet varying cooling loads, and include such strategies as simple on/off control, compressor cylinder unloading, and variable speed compressor control. A summary of theoretical and experimental studies to determine the best capacity control method was conducted by Qureshi and Tassou in 1996 [1]. They found that both theoretical and experimental analyses demonstrated that variable speed compressor control provided the greatest flexibility to match heat loads, resulting in the best overall system efficiency. In many of the papers they summarized, the variable speed control strategies resulted in 20% to 40% reductions in seasonal power consumption. However, in order to effectively manage variable speed compressor systems it is critical that the control architecture is properly designed. In particular, the coordination of the compressor speed with other mass flow control devices is very important.

It should be noted that this work focuses on the control of the vapor compression cycle (VCC) itself; that is, the working of the refrigerant about some cycle such as shown in Figure 1. This cycle depicts the energy exchange done on a refrigerant fluid as it is compressed and expanded.

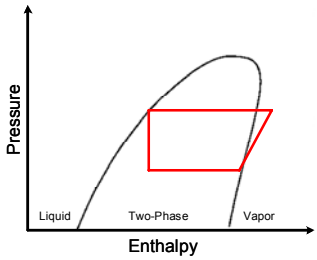

Figure 1 - A standard VCC Pressure-enthalpy (P-h) diagram

This cycle forms the basis for energy transfer and, in effect, becomes a critical inner loop to other higher level planning algorithms focused on overall outer loop control and optimization for enclosed environments such as [2]. In general, VCC systems are controlled to maximize the energy efficiency of the system while ensuring the fluid entering the compressor is in the vapor phase [3]. If liquid enters the compressor it can cause a variety of system problems, including decreased efficiency, disruptions to oil circulation, and physical damage to compressor components. To prevent liquid from entering the compressor, vapor compression systems are designed to operate with a certain degree of superheat, defined as the temperature the exiting refrigerant is above the saturation temperature at the evaporator outlet. A block diagram of a standard variable speed capacity control configuration commonly found in the air-conditioning and refrigeration industry is presented in Fig. 2. This is a schematic of the experimental system described in Section II. The reader should note the existence of an electronic expansion valve (EEV) as a second controllable mass flow device in Figure 2.

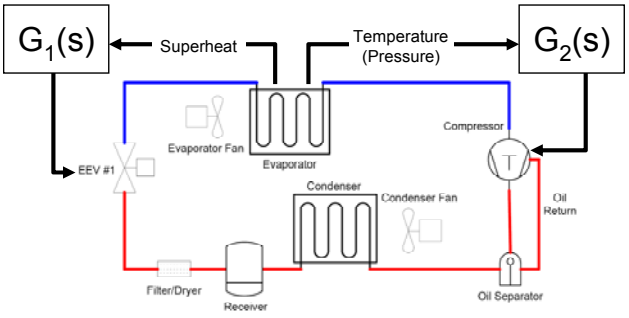

Figure 2 - A standard control approach for vapor compression systems

To control the cooling capacity provided by the evaporator it is common to use the evaporator temperature in any type of feedback controller. In this

M. C. Keir received his M.S. Degree from the University of Illinois at Urbana-Champaign, Urbana, IL 61801 USA. (email: mckeir@gmail.com)

A. G. Alleyne is a Professor at University of Illinois at Urbana-Champaign, Urbana, IL 61801 USA (phone: 217-244-9993; fax: 217-244-6534; email: alleyne@uiuc.edu).

work however, we exercise the freedom of substituting a mean evaporator pressure as a substitute for evaporator wall temperature. The motivation for this is that the two quantities can be closely correlated and the speed of response of evaporator refrigerant pressure is much faster than that of an evaporator wall temperature. This effectively increases the bandwidth of the output sensor.

The combination of the desire to match external heat loads (capacity control) with the internal refrigerant phase limitations (superheat regulation) necessary for system efficiency requires that the control system simultaneously meet multiple control objectives. The controllers $G_1(s)$ and $G_2(s)$ in Fig. 2 are usually basic SISO algorithms designed independently [6]. Since the dynamics of the system are inherently coupled, it is critical to find appropriate system signals that can be used in a multivariable manner to effectively manage the system. This paper provides a detailed discussion of standard and alternative controller feedback configurations in order to develop a simple control framework that achieves high performance while retaining a degree of simplicity that makes the method practical in many industrial applications.

The remainder of this paper is organized as follows. Section II describes the experimental system used for the analysis presented in this paper. Section III provides a discussion of the traditional feedback configuration found in the literature. Section IV explores the open loop plant dynamics and coupling within vapor compression systems. Section V presents an example of the use of two feedback configurations on an experimental system. Finally, Section VI concludes by highlighting the benefit of the alternative controller configuration.

II. Experimental System Description

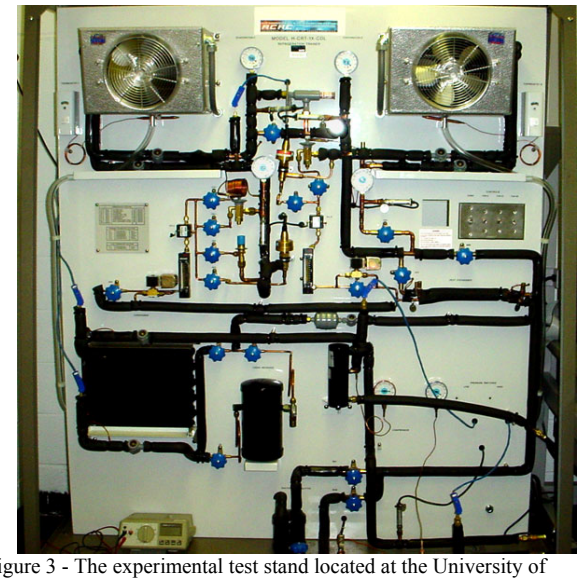

Figure 3 - The experimental test stand located at the University of Illinois at Urbana-Champaign

The results presented in this section were taken from a small experimental test stand at the University of Illinois at Urbana-Champaign. The test stand has the potential to mimic the behavior of a variety of vapor compression system configurations. The experimental system has a semi-hermetic reciprocating compressor, a single condenser, an array of expansion devices, two evaporators and an internal heat exchanger. The system contains sufficient bypasses and valves to allow the system to be configured in a single or dual evaporator format with the choice of a thermal expansion valve (TXV), orifice tube, automatic expansion valve, or an electronic expansion valve (EEV) regulating the mass flow of the system.

The system has five controllable inputs available, if needed, for any type of feedback algorithm; compressor speed, EEV valve opening, both evaporator fan speeds, and the condenser fan speed. The system is fully instrumented with 6 pressure gauges, 2 mass flow meters, and 24 thermocouples. A complete description of the system can be found in [3]. For the experimental results presented in this paper the system was placed in a single evaporator configuration that bypassed the internal heat exchanger. The EEV was used as the expansion device for improved controllability. A block diagram of the configuration used for the experimental results was presented in Fig. 2. A picture of the actual experimental system is presented in Fig. 3.

III. Classical Variable Speed Control

From the point of view of the refrigerant cycle, the two control goals of a VCC system are to prevent liquid ingestion in the compressor (superheat regulation) and to match the heat load of the cooled space. Recently, the development of low order dynamic models of vapor compression systems has enabled the application of advanced control techniques [3,4]. As an example, a model developed in [4] provides a system model with the state space form given in Eq. 1, with the states, inputs and outputs listed in Eqs. 2-4. Where l_e is the length of the two phase section in the evaporator, P_e is the evaporator pressure, T_{we} is the wall temperature in the evaporator, P_c is the condenser pressure, T_{wc} is the condenser wall temperature, ω_c is the compressor speed, a_v is the valve opening, T_e is the saturation temperature in the evaporator, and SH is the superheat at the evaporator exit.

$$\dot{\mathbf{x}} = \mathbf{A}\mathbf{x} + \mathbf{B}\mathbf{u} \qquad \mathbf{y} = \mathbf{C}\mathbf{x} + \mathbf{D}\mathbf{u} \tag{1}$$

$$\mathbf{x} = \begin{bmatrix} l_e & P_e & T_{we} & P_c & T_{wc} \end{bmatrix}^T \tag{2}$$

$$\mathbf{u} = \begin{bmatrix} \omega_c & a_v \end{bmatrix}^T \tag{3}$$

$$\mathbf{y} = \begin{bmatrix} T_e & SH \end{bmatrix}^T \tag{4}$$

Clearly, even with this relatively simple model, the number of sensors required to use standard state feedback control approaches is unacceptably high. In [4] the system superheat and evaporator saturation temperature were

used as the measured outputs supplied to an optimal observer to estimate the system state (LQG). Numerous other control schemes have been developed with superheat and evaporation temperature (or pressure) as the feedback signals [3,4,5,6]. These references frequently noted the difficulty of controlling the two outputs with a decentralized controller configuration (individual SISO control loops) due to the physical coupling between superheat and evaporation temperature.

The feedback configuration used in [3,4,5,6] is not the only possible approach. We consider two primary controllable inputs for a variable speed vapor compression systems; the compressor speed and the valve opening. While controllable fan speeds to regular air mass flow rate are also inputs in certain cases, we do not consider them here as inputs. This is due to the fact that in some cases, e.g. automotive systems, the condenser airflow rate is a function of vehicle speed and acts almost as a disturbance to the feedback loop. In all cases the superheat of the system must be regulated, but here the pressure of the evaporator is selected as a regulated system output because of its relationship to the saturation temperature which is subsequently related to system cooling capacity. There are a variety of other signals that exhibit the proper characteristics to be effectively used to modulate the cooling capacity of the system and some of those not presented here are explored in [6].

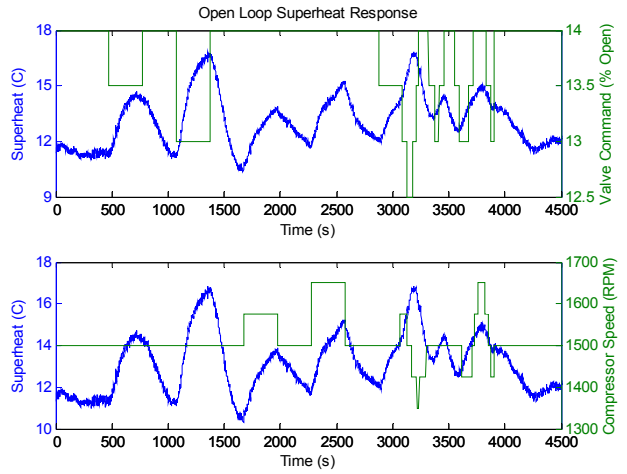

Fig. 4 - Open loop superheat response to a series of valve and compressor steps

The basic dynamic response of a vapor compression system can be identified using a simple time domain system identification procedure. Initially the output responses to valve steps, compressor steps and pseudo-random binary combinations of compressor and valve steps around a nominal operating condition of 1500 RPM were collected. Figures 4 and 5 depict the response of the system superheat and evaporator pressure with the input signals overlaid on the response. For compactness of comparison, both the input (right axis) and the output (left axis) are given on the same plot. The stepwise data without noise would be the input signals. Figures 4 and 5 demonstrate that both valve and compressor steps have a significant impact on the response of superheat and evaporator pressure, implying a strong internal coupling between the responses of the two outputs. The internal coupling indicates that the system will be difficult to control, and to achieve high performance system regulation advanced multivariable control techniques are required [3,4].

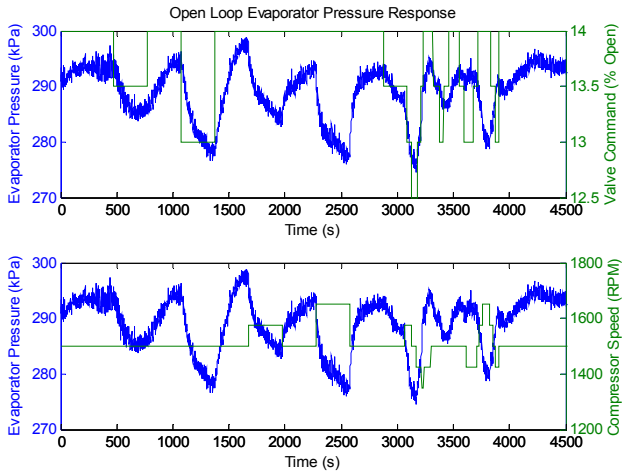

Fig. 5 - Open loop evaporator pressure response to a series of valve and compressor steps

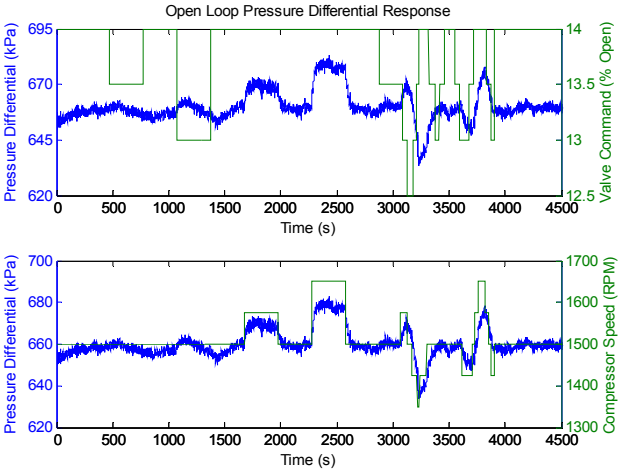

Fig 6 - Open loop pressure differential response to a series of valve and compressor steps

An alternative to applying advanced multivariable control techniques is to explore the use of another signal in the feedback path that is not as highly coupled to the superheat of the system. One signal that exhibits all of the right characteristics is the pressure differential across the refrigerant system loop: $\Delta P = P_{condenser} - P_{evaporator}$. An increase in the operating pressure differential, when the superheat of the system remains constant, is caused by an increase in compressor speed that results in a higher mass flow rate of refrigerant through the system. Therefore, pressure differential (or difference in saturation temperatures) across the vapor compression system would

serve as a good indicator of system capacity, providing an alternative signal to use in the feedback path. Figure 6 depicts the time domain ΔP response of the vapor compression system to the valve and compressor steps. From Fig. 6, it is readily apparent that the pressure differential of the system responds much more significantly to changes in compressor speed than valve steps, implying a decrease in coupling for this output.

IV. An Alternative Feedback Configuration

The benefits of using the system ΔP in place of a single pressure (or saturation temperature) are explored in the following. The proposed change to the feedback configuration can be seen by comparing the feedback configuration presented in Fig. 7 to that shown in Fig. 2.

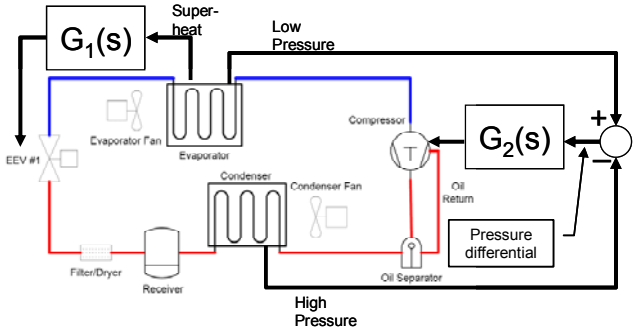

Figure 7 - Alternative feedback configuration for control design

As can be seen in the figure, the compressor controller is now driven by the pressure difference across the system. This is intuitively natural since the compressor acts to change the pressure difference between the evaporator and condenser rather than acting to change one of the heat exchanger pressures in isolation.

One metric that can be used to quantify the reduction in coupling provided by using the system pressure differential in place of the evaporator pressure in the feedback path is a relative gain array (RGA) technique originally developed by Bristol [7]. To apply the RGA analysis, a dynamic model of the system must be identified using the time domain data. For the purpose of illustration, the models used here are lower order than those described in Equations (1)-(4). Using a standard prediction error/maximum likelihood system identification procedure [8], a second order dynamic model with superheat and either evaporator pressure or pressure differential as outputs can be identified. The identified state space **[A,B,C,D]** superheat/evaporator pressure system model is given in Eq. 5.

$$A=\begin{bmatrix}-0.0039 & -0.0057\\ 0.013 & -0.048\end{bmatrix}\quad B=\begin{bmatrix}-0.00017 & -2.2e-6\\ 0.0021 & -3.3e-5\end{bmatrix}$$
$$C=\begin{bmatrix}80 & -8.6\\ -193 & 104\end{bmatrix}\quad D=\begin{bmatrix}0 & 0\\ 0 & 0\end{bmatrix} \qquad (5)$$
$$\mathbf{u}=\begin{bmatrix}\omega_c & a_v\end{bmatrix}^T\quad \mathbf{y}=\begin{bmatrix}P_{evaporator} & SH\end{bmatrix}^T$$

The identified superheat/pressure differential system model is given in Eq. 6.

$$A=\begin{bmatrix}-0.0052 & -0.00016\\ -0.010 & -0.041\end{bmatrix}\quad B=\begin{bmatrix}-0.00044 & -2.2e-6\\ 0.0011 & -3.1e-5\end{bmatrix}$$
$$C=\begin{bmatrix}81 & -0.16\\ -57 & 202\end{bmatrix}\quad D=\begin{bmatrix}0 & 0\\ 0 & 0\end{bmatrix} \qquad (6)$$
$$\mathbf{u}=\begin{bmatrix}\omega_c & a_v\end{bmatrix}^T\quad \mathbf{y}=\begin{bmatrix}\Delta P & SH\end{bmatrix}^T$$

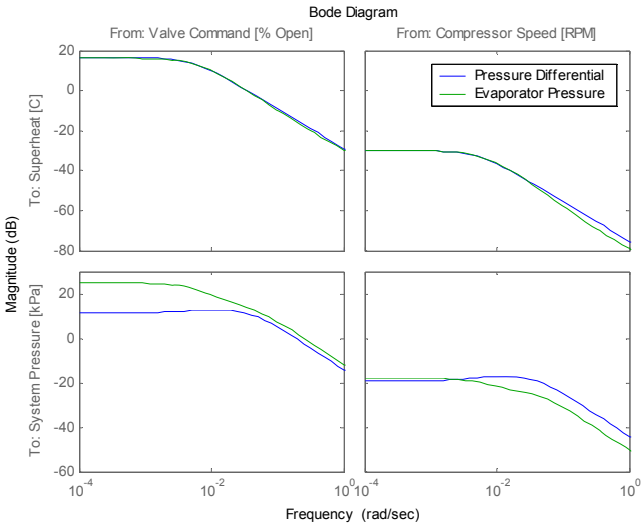

Figure 8 - Bode magnitude response of the two identified system models

The magnitude frequency response of the two identified system models is provided in Fig. 8. The main difference indicated in Fig. 8 is that the valve-to-ΔP transfer function has a significantly lower magnitude than the valve-to-$P_{evaporator}$ transfer function, indicating a reduction in coupling. The RGA is a steady-state measure of closed loop interactions for decentralized (multiple SISO loop) control. For a non-singular square matrix, P, the relative gain array is defined by Eq. (7), where × denotes element by element multiplication (Schur product).

$$RGA(P)=\Lambda(P)=P\times\left(P^{-1}\right)^T \qquad (7)$$

The RGA is a good indicator of [9]:

- sensitivity to uncertainty in the input channels
- diagonal dominance
- the stability of decentralized control

Uncertainty in the input channels is indicated by plants with large RGA elements around the crossover frequency, making these plants fundamentally difficult to control. A measure of the diagonal dominance of a plant, G, is obtained by calculating the RGA-number, given in Eq. (8).

$$RGA-number(G(\omega))=\left\|\Lambda(|G(\omega)|)-I\right\|_{sum} \qquad (8)$$

Large RGA numbers are a clear indicator that the closed loop performance will be poor when decentralized control schemes are applied [9]. Figure 9 contains a plot the RGA-number vs. frequency for both feedback

configurations. Clearly, the model with evaporator pressure as an output given in (5) has a significantly higher RGA-number at all frequencies. This indicates that the superheat/$P_{evaporator}$ model has a higher degree of coupling between the controlled outputs.

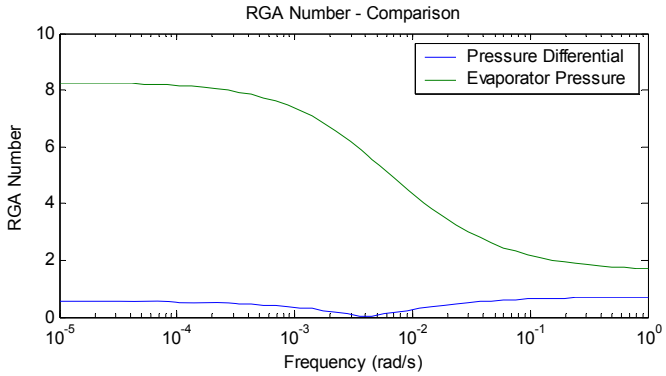

Figure 9 - Plot of the RGA-number vs. frequency for the two identified system models

It is interesting to note that the RGA-number drops towards zero at a frequency of 0.004 rad/s in the superheat/ΔP model from Eq. (6). This due to the plant becoming triangular as the system pressure differential becomes unresponsive to changes in valve position. This implies higher frequency valve movements will not significantly impact the system pressure differential, resulting in a nearly triangular plant that would be significantly easier to control using decentralized control approaches.

V. Decentralized PID Example

Assume that G_1 and G_2 from Figs. 2 and 7 represent a PID and a PI controller respectively. This is a reasonable assumption given that the majority of industrial controllers for these types of systems, with continuously variable inputs, would use some type of PID algorithm to close the loop. Using the identified models for the superheat/evaporator pressure and superheat/pressure differential output configurations, the PID controllers were tuned in simulation to obtain a closed loop system performance with a rise time of approximately 25 seconds and a settling time less than 100 seconds to a step change in the pressure reference. The size of the pressure reference change was selected to require a comparable level of change in the compressor speed (~80 RPM) regardless of the magnitude of the pressure feedback signal. The gains for the superheat/$P_{evaporator}$ controller of Fig. 2 are given in Eq. (9).

$$P_{G1} = 4 \quad I_{G1} = 0.01 \quad D_{G1} = 4 \quad P_{G2} = 22 \quad I_{G2} = 2.25 \quad (9)$$

The gains for the superheat/ΔP controller shown in Fig. 7 are given in Eq. (10).

$$P_{G1} = 2 \quad I_{G1} = 0.01 \quad D_{G1} = 4 \quad P_{G2} = 12 \quad I_{G2} = 0.85 \quad (10)$$

The benefits of the ΔP control feedback structure can be analyzed by exploring differences between the two controllers that are tuned to obtain similar performance. Figure 10 depicts a set of possible exogenous signals that could be used to explore closed loop sensitivity, where d is a disturbance, r is the reference, n is sensor noise, F is a low pass filter, K is the controller, and G is the plant. Equations (11)-(14) present the sensitivity functions corresponding to Fig. 10. The most significant difference between the two feedback configurations is in the sensitivity to noise, shown in Fig. 11. It is clear that the system with ΔP feedback has a much lower output disturbance sensitivity than the system with a single pressure (or saturation temperature) feedback. This reduced feedback sensitivity greatly increases the closed loop performance, particularly at lower frequencies. The full analysis of the closed loop sensitivity functions is presented in [6].

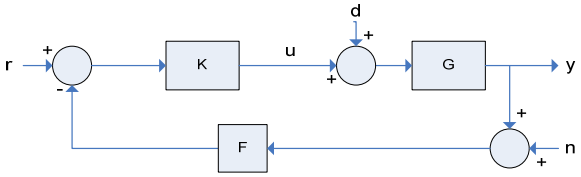

Fig. 10 - Potential exogenous signals that can be included in a sensitivity analysis

$$\frac{y}{r} = (I + GKF)^{-1} GK \quad (9)$$

$$\frac{y}{d} = (I + GKF)^{-1} G \quad (10)$$

$$\frac{y}{n} = (I + GKF)^{-1} GKF \quad (11)$$

$$\frac{u}{n} = -(I + KFG)^{-1} KF \quad (12)$$

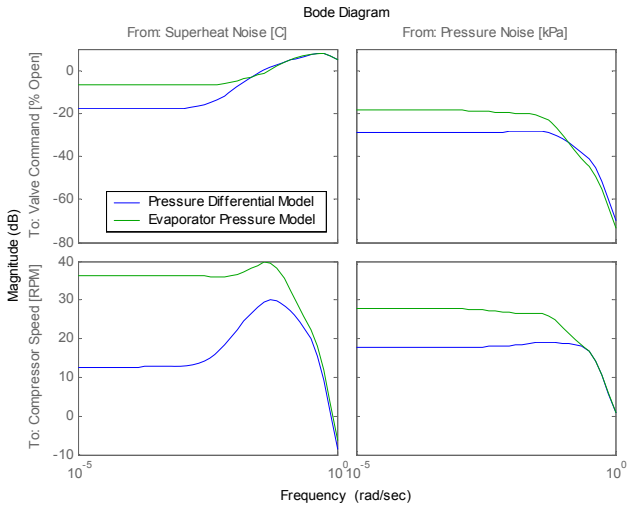

Figure 11 - Bode magnitude plot of the noise sensitivity for the two controllers

The experimental performance of the two controllers is summarized in Figs. 12 and 13. Note that similar operating conditions are used but the resulting magnitude of ΔP is larger than $P_{evaporator}$ since it is a difference in pressures. The reference command changes given in Figs.

12 and 13 illustrate changes given in capacity while regulating superheat. Comparing the results in parts a) and b) of Figs. 12 and 13, it is clear that the controller with evaporator pressure as a controlled variable oscillates around the pressure set point. This becomes readily apparent when comparing the finer time scale pressure response to a reference step, shown in part d). The superheat/ΔP controller settles at the new set point in about 25 seconds, whereas the superheat/$P_{evaporator}$ response takes approximately 40 seconds just to reach the new set point with persistent oscillations that decay slightly over the next 100 seconds.

The fighting that results from the coupled superheat/$P_{evaporator}$ dynamics is perhaps best illustrated by comparing the actuator signals shown in parts e) and f) of Figs. 12 and 13. The compressor speed and valve actuation required by the superheat/$P_{evaporator}$ controller oscillate considerably after the initial step, whereas the reduced coupling of the superheat/ΔP feedback configuration results in non-oscillatory actuation. In practice, the reduced actuation should lead to less wear on system components such as the compressor and EEV.

It should be noted that although the superheat/ΔP controller obtains better regulation, part c) indicates that the controller still induced small initial oscillations in system capacity instead of cleanly transitioning to a new set point. The use of more coordinated control strategies enables the designer to eliminate the oscillations in capacity while retaining the high performance regulation of superheat and pressure differential [6].

VI. Conclusions

As the limits of system efficiency are pressed by the conversion of AC&R systems to continuous operation configurations, it is imperative that the systems employ the proper controller architecture to effectively regulate the desired system outputs. This paper demonstrates that an appropriate choice of feedback variables, or closed loop structure, can have large effects on system behavior. By system, we mean the closed loop control of the refrigeration cycle that could be a part of an overall energy management scheme. The (ΔP) framework presented here for the first time, demonstrated 2 significant advantages. First, the system with (ΔP) feedback had greatly reduced output sensitivity compared with a more traditional feedback scheme of evaporator pressure (or saturation temperature). Secondly, the MIMO system input-output coupling was greatly reduced with (ΔP) feedback compared with a more traditional feedback scheme of evaporator pressure (or saturation temperature).

The decrease in system coupling exhibited by the superheat/ΔP feedback configuration vastly improves decentralized controller performance, as demonstrated in Section V. The decentralized controller for the superheat/pressure differential feedback configuration obtained better output tracking because of the reduced fighting between the individual control loops, producing relatively smooth steps in system capacity without creating oscillatory responses in system actuation.

In closing, it should be noted that the analysis performed here to determine less coupled feedback structures is performed for a linear system representation. VCC systems are actually very nonlinear systems. Any linear VCC system representation will vary greatly in its parameters about different operating points [10]. However, linearizing the system about any operating point and performing a local analysis will result in a similar type of decoupling benefit to the ΔP approach. The precise nature of the dynamic decoupling will be dependent on the system parameters used in the local linear representation but the general phenomenon should be the same.

Acknowledgment

This work was supported in part by the sponsoring companies of the Air-Conditioning and Refrigeration Center at the University of Illinois at Urbana-Champaign.

References

[1] Qureshi, T. Q. and Tassou, S. A., "Variable-speed capacity control in refrigeration systems," *Applied Thermal* Engineering, vol. 16, no. 2, pp. 103-113, 1996.

[2] Larsen, L., Thybo, C., Stoustrup, J., Rasmussen, H., "A Method for Online Steady State Energy Minimization with Application to Refrigeration Systems," *Proc of the 43rd IEEE CDC*, pp. 4708-4713, Bahamas, Dec. 2004.

[3] Rasmussen, B. P., "Dynamic Modeling and Advanced Control of Air Conditioning and Refrigeration Systems," Phd. Dissertation, Dept. of Mechanical Engineering, University of Illinois at Urbana-Champaign, 2005.

[4] He, X. D., Liu, S., and Asada, H., "Multivariable Control of Vapor Compression Systems," *HVAC&R Research*, vol. 4, pp. 205-230, 1998.

[5] Shah, R., Rasmussen, B., Alleyne, A., "Application of Multivariable Adaptive Control to Automotive Air Conditioning Systems," *International Journal of Adaptive Control and Signal Processing*, Vol. 18, No. 2, pp. 199-221, March 2004.

[6] Keir, M. C., "Dynamic Modeling, Control, and Fault Detection in Vapor Compression Systems," MS Thesis, Dept. of Mechanical Engineering, University of Illinois at Urbana-Champaign, 2006.

[7] Bristol, E. H., "On a new measure of interaction for multi-variable process control," *IEEE Transactions on Automatic Control*, vol. 11, no. 1, pp. 133-134.

[8] Ljung, L., *System Identification Toolbox: For Use with Matlab*, The Math Works Inc., Natick, MA, 2001.

[9] Skogestad, S., and Postlethwaite, I., *Multivariable Feedback Control*, John Wiley & Sons, New York, 1996.

[10] Rasmussen, B. and A. Alleyne, "Gain Scheduled Control of an Air Conditioning System Using the Youla Parameterization," *2006 American Control Conference*, Minneapolis, MN, pp. 5336-5341, June 14-16, 2006.

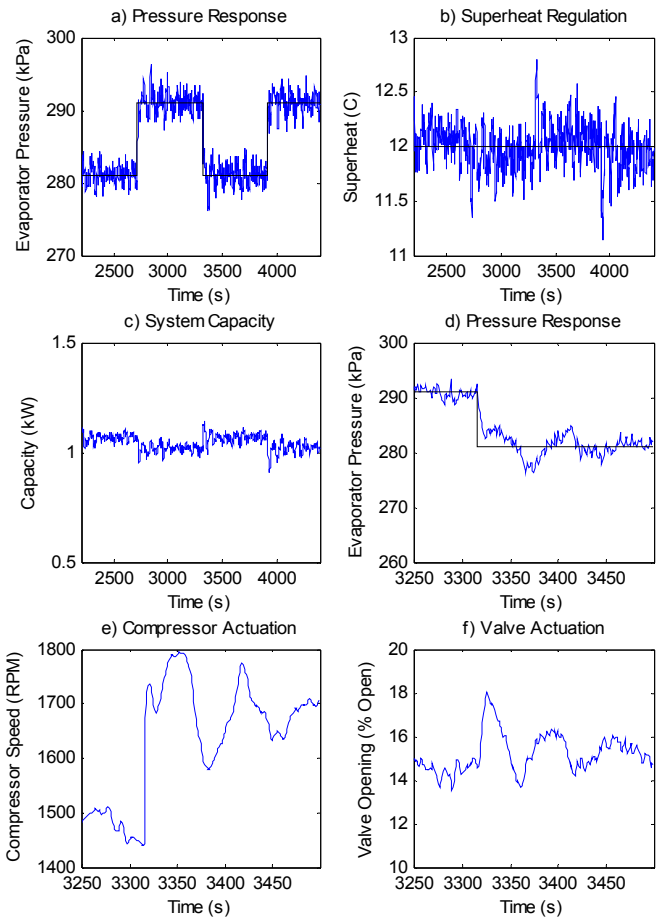

Figure 12 - Performance of the superheat/$P_{evaporator}$ controller

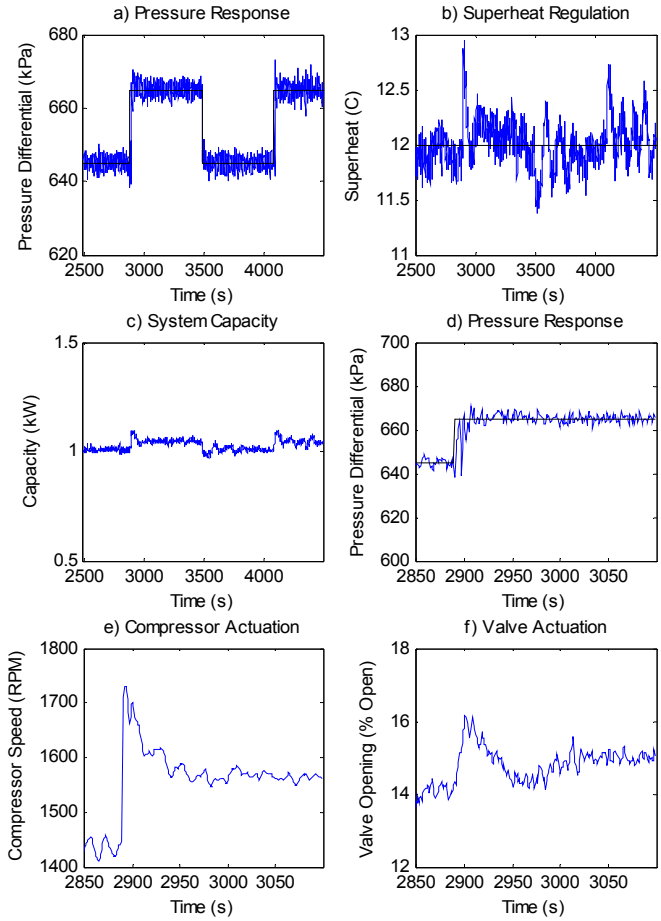

Figure 13 - Performance of the superheat/ΔP controller.